MoM/BI–RME Analysis of Boxed MMICs With Arbitrarily Shaped Metallizations

Maurizio Bozzi, *Member, IEEE*, Luca Perregrini, *Member, IEEE*, Alejandro Alvarez Melcón, *Member, IEEE*, Marco Guglielmi, *Senior Member, IEEE*, and Giuseppe Conciauro, *Member, IEEE*

***Abstract*—In this paper, we propose a novel approach for the analysis of shielded microstrip circuits, composed of a number of thin metallic areas with arbitrary shapes and finite conductivity, embedded in a multilayered lossy medium. The analysis is based on the solution of an integral equation (IE) obtained by enforcing the proper boundary condition to the electric field on the metallic areas. The IE is solved by using the method of moments with entire domain basis functions, which are numerically determined by the boundary integral-resonant-mode expansion (BI–RME) method. The use of the BI–RME method allows for the efficient calculation of the basis functions independently on the shape of the domain, thus permitting the analysis of a wide class of circuits. Two examples demonstrate the accuracy, rapidity, and flexibility of the proposed method.**

***Index Terms*—Entire domain basis functions, integral equations, microstrip filters, MMICs, moment method.**

I. Introduction

OVER THE last years, considerable interest has been directed to the design of boxed multilayered circuits (Fig. 1). This configuration is typically considered in the design of many actual monolithic microwave integrated circuits (MMICs), both in single-layer [1] and multilayered configurations [2], [3].

Among the possible numerical methods applied to the analysis of this type of structures, the integral equation (IE) method is by far one of the most efficient. The IE method can be formulated either in the spectral [4] or spatial domains [5]. The resulting IE is solved by the method of moments (MoM), usually considering sub-domain basis functions (e.g., rooftops [6], [7] or basis functions on triangular domains [8], [9]).

Recently, the IE/MoM method in the spectral domain was applied with entire domain basis functions [10]. The main advantage of using the vector modal functions derived in [10] is the dramatic reduction in the order of the MoM matrix since few entire domain basis functions are usually sufficient to represent the unknown currents. Moreover, the calculation of the MoM matrix is enhanced because of the rapid decrease of the spectral components to be added subsequently for the calculation of the matrix elements. It is noted, however, that the original work derived in [10] is limited to areas with a rectangular shape, where the entire domain basis functions are known analytically.

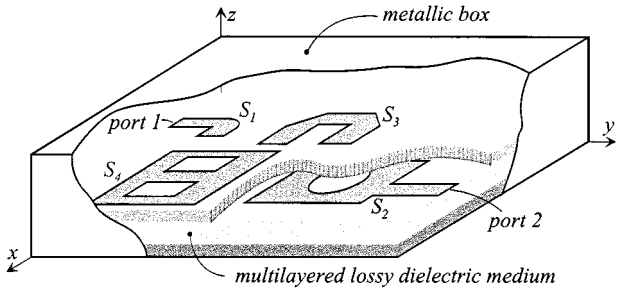

Fig. 1. Shielded MMIC with arbitrarily shaped metallic areas in a multilayered lossy medium. The patches can be placed at different height and they may overlap.

In this paper, we present the extension of the method proposed in [10] to the case of metallic areas with an arbitrary shape (Fig. 1). The entire domain basis functions are determined numerically by the boundary integral-resonant mode expansion (BI–RME) method [11]. The use of the BI–RME method has two main advantages. The first is the possibility of obtaining entire domain basis functions for arbitrary shapes in a short time, and the second is that the entries of the MoM matrix are practically obtained as a by-product of the method itself. In fact, the surface integrals involved in the calculations of the MoM matrix can be converted into line integrals on the boundary of the metallic areas, and the quantities required on the boundary are the basic output of the BI–RME calculation.

A preliminary discussion of the proposed algorithm was presented in [12]. This paper gives a comprehensive explanation of the MoM/BI–RME method, adding two novel capabilities: metallic areas including a port may have an arbitrary shape, and multiply connected metallizations can be considered.

II. IE/MoM Approach

Let us consider the structure shown in Fig. 2, consisting of a multilayered medium and P metallic areas with arbitrary shapes $S_1, \ldots, S_P$, possibly located at different interfaces. The circuit is fed at the frequency ω at K ports ($K \leq P$), conventionally defined on the first K areas $S_1, \ldots, S_K$. As usual [5], [13], [14], the ports are represented as small gaps between the metallization and the wall of the box (delta-gap voltage excitations).

Manuscript received March 30, 2001; revised August 9, 2001. This work was supported by the European Commission under Project MMCODEF, under Contract HPRN-2000-00043, and by the Consiglio Nazionale delle Ricerche under Contract MADESS II.

M. Bozzi, L. Perregrini, and G. Conciauro are with the Department of Electronics, University of Pavia, 27100 Pavia, Italy (e-mail: maurizio.bozzi@ele.unipv.it; luca.perregrini@ele.unipv.it; giuseppe.conciauro@ele.unipv.it).

A. Alvarez Melcón is with the Department of Information Technologies and Communications, Technical University of Carthagene, 30202 Cartagena, Spain (e-mail: alejandro.alvarez@upct.es).

M. Guglielmi is with the European Space Research and Technology Center, European Space Agency–European Space Research and Technology Centre, 2200AG Noordwijk, The Netherlands (e-mail: marco.guglielmi@esa.int).

Publisher Item Identifier S 0018-9480(01)10474-6.

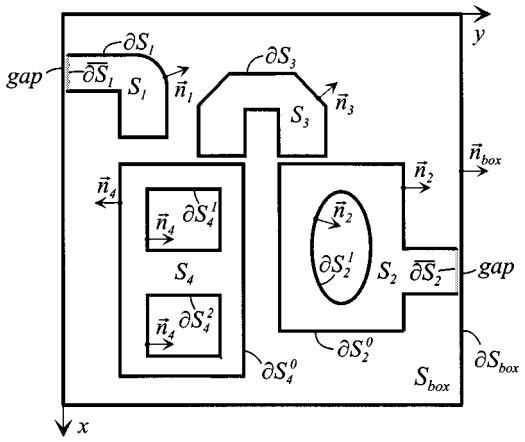

Fig. 2. Different metallic areas considered in the analysis: simply (S_1) or multiply connected patches attached to a port (S_2), simply (S_3) or multiply connected internal patches (S_4). ∂S_p represents the boundary of the area S_p, except the possible part corresponding to a port (denoted by $\overline{\partial S}_p$). In case of multiply connected areas, ∂S_p consists of many lines ∂S_p^0, ∂S_p^1, ...

In [10], the analysis is based on the solution of a system of P IEs, which are obtained by enforcing the boundary condition to the transverse-to-z electric field at all the metallic areas

$$Z\vec{J}_p(\vec{r}) - \sum_{q=1}^{P} \int_{S_q} \overleftrightarrow{G}(\vec{r}, \vec{r}'|\omega) \cdot \vec{J}_q(\vec{r}')\, dS' = \begin{cases} -\vec{n}_p v_p \delta(\vec{r}, \vec{r}_p)|_{\vec{r}_p \in \overline{\partial S}_p}, & p = 1, \ldots, K \\ 0, & p = K+1, \ldots, P \end{cases} \quad (1)$$

where the points $\vec{r}$ and $\vec{r}'$ belong to S_p and S_q, respectively, $\overline{\partial S}_p$ denotes the part of the boundary of S_p that belongs to the pth port, $\vec{n}_p$ is the outward normal, v_p is the voltage applied to the pth port, and Z is the "sheet impedance" of the metallizations. The choice of Z is problem dependent. For instance, in the case of a single-layer microstrip circuit with a metallization thickness t much larger than the skin depth δ, we can use the surface impedance of the conductors $Z = Z_s = (1+j)\rho/\delta$ (ρ is the resistivity of the metal), in the case of low-frequency calculations ($t \ll \delta$), we can use $Z = \rho/t$. Moreover, $\vec{J}_q$ is the (unknown) current density on S_q, and the Green's function $\overleftrightarrow{G}$ is given by [15]

$$\overleftrightarrow{G}(\vec{r}, \vec{r}'|\omega) = \sum_m V_m(z, z'|\omega)\vec{\mathcal{E}}_m(x, y)\vec{\mathcal{E}}_m(x', y') \quad (2)$$

where $\vec{\mathcal{E}}_m$ are the transverse electric modal vectors of the TE and TM modes of the box, with the normalization $\int_{S_{box}} |\vec{\mathcal{E}}_m|^2\, dS = 1$. The expressions of $\vec{\mathcal{E}}_m$ are

$$\vec{\mathcal{E}}'_m = -\frac{\nabla_T \chi'_m}{k'_m} \quad \text{(TM modes)} \quad (3)$$

$$\vec{\mathcal{E}}''_m = -\vec{u}_z \times \frac{\nabla_T \chi''_m}{k''_m} \quad \text{(TE modes)} \quad (4)$$

where χ'_m and χ''_m are the eigenfunctions of the Helmholtz equation with the Dirichlet or Neumann boundary conditions on ∂S_{box} (see Fig. 2), and k'_m and k''_m are the corresponding eigenvectors. Finally, functions V_m are determined by considering the equivalent modal transmission lines for the layered box [10], [16].

Equation (1) is solved by applying the MoM in the Galerkin form. The unknown current density $\vec{J}_p$ is represented through a suitable set of N_p basis functions $\vec{e}_r^{(p)}$ defined on the pth patch, namely,

$$\vec{J}_p = \sum_{r=1}^{N_p} \xi_r^{(p)} \vec{e}_r^{(p)}, \qquad p = 1, \ldots, P \quad (5)$$

where $\xi_r^{(p)}$ are unknown coefficients.

As discussed in [10], the calculation of the MoM matrices involves frequency-independent coefficients of two types. The former represents the *coupling integral* between the rth basis function on the pth metallic area and the mth modal vector of the box, and is given by

$$\mathcal{C}_{rm}^{(p)} = \int_{S_p} \vec{e}_r^{(p)}(\vec{r}) \cdot \vec{\mathcal{E}}_m(\vec{r})\, dS. \quad (6)$$

The latter is the projection of the delta-gap excitation of the pth port on the rth basis function (*port integral*), and is given by

$$\mathcal{P}_r^{(p)} = \int_{\overline{\partial S}_p} \vec{e}_r^{(p)}(\vec{r}) \cdot (-\vec{n}_p)\, d\ell. \quad (7)$$

For any frequency, the scattering parameters are calculated straightforwardly from the coefficients $\xi_r^{(p)}$ obtained by the solution of the MoM system [10].

III. Entire Domain Basis Functions

A key feature of the present approach is the use of a set of entire domain basis functions, i.e., functions $\vec{e}_r^{(p)}$, which span the entire domain S_p.

The advantage of using such functions has been demonstrated in [10], with reference to the case where all surfaces S_p are rectangular. More specifically, the electric modal vectors of rectangular waveguides bounded by magnetic or mixed-type walls have been used as basis functions. In this paper, the same concept is applied to metallization of arbitrary shapes, with no restriction on the geometry of the surfaces S_p. In this case, the basis functions must be determined numerically and the efficiency of the numerical method used for their calculation is a vital issue. The BI–RME method discussed in Section V permits to determine very efficiently enough basis functions for our application.

In the case of simply connected surfaces, we have to calculate two classes of basis functions expressed by

$$\vec{e}_r^{\,\prime(p)} = -\vec{u}_z \times \frac{\nabla_T \psi_r^{\prime(p)}}{\kappa_r^{\prime(p)}} \quad (8)$$

$$\vec{e}_r^{\,\prime\prime(p)} = -\frac{\nabla_T \psi_r^{\prime\prime(p)}}{\kappa_r^{\prime\prime(p)}} \quad (9)$$

where the pairs $\{\psi_r'^{(p)}, \kappa_r'^{(p)}\}$ and $\{\psi_r''^{(p)}, \kappa_r''^{(p)}\}$ are the eigensolutions of the homogeneous Helmholtz equation in the domain S_p, i.e.,

$$\nabla_T^2 \psi_r'^{(p)} + \kappa_r'^{(p)^2} \psi_r'^{(p)} = 0, \qquad \text{in } S_p \tag{10}$$

$$\nabla_T^2 \psi_r''^{(p)} + \kappa_r''^{(p)^2} \psi_r''^{(p)} = 0, \qquad \text{in } S_p. \tag{11}$$

In the case of N-times connected surfaces, the set of basis functions must be supplemented with $N-1$ additional functions

$$\vec{e}_r^{\,0(p)} = -\vec{u}_z \times \nabla_T \psi_r^{0(p)} \tag{12}$$

where $\psi_r^{0(p)}$ satisfies the Laplace equation in the domain S_p, i.e.,

$$\nabla_T^2 \psi_r^{0(p)} = 0, \qquad \text{in } S_p. \tag{13}$$

The boundary conditions are different for metallizations connected or not connected to ports.

In the case of metallizations not connected to ports (e.g., S_3 and S_4 in Fig. 2), $\vec{J}_p$ is tangent to the whole boundary of S_p. The basis functions $\vec{e}_r'^{(p)}$, $\vec{e}_r''^{(p)}$, and $\vec{e}_r^{\,0(p)}$ satisfy the same boundary condition provided that

$$\psi_r'^{(p)} = 0, \qquad \text{on } \partial S_p \tag{14}$$

$$\partial \psi_r''^{(p)} / \partial n_p = 0, \qquad \text{on } \partial S_p \tag{15}$$

$$\psi_r^{0(p)} = \begin{cases} 1, & \text{on the inner contour } \partial S_p^i \\ 0, & \text{on } \partial S_p - \partial S_p^i. \end{cases} \tag{16}$$

In the case of metallizations connected to ports (e.g., S_1 and S_2 in Fig. 2), $\vec{J}_q$ is perpendicular to the port segment $\overline{\partial S}_p$. In this case, $\psi_r'^{(p)}$, $\psi_r''^{(p)}$, and $\psi_r^{0(p)}$ must satisfy the mixed boundary conditions

$$\begin{cases} \psi_r'^{(p)} = 0, & \text{on } \partial S_p \\ \partial \psi_r'^{(p)} / \partial n_p = 0, & \text{on } \overline{\partial S}_p \end{cases} \tag{17}$$

$$\begin{cases} \partial \psi_r''^{(p)} / \partial n_p = 0, & \text{on } \partial S_p \\ \psi_r''^{(p)} = 0, & \text{on } \overline{\partial S}_p \end{cases} \tag{18}$$

$$\begin{cases} \psi_r^{0(p)} = \begin{cases} 1, & \text{on the inner contour } \partial S_p^i \\ 0, & \text{on } \partial S_p - \partial S_p^i \end{cases} \\ \partial \psi_r^{0(p)} / \partial n_p = 0, & \text{on } \overline{\partial S}_p. \end{cases} \tag{19}$$

It is worthy noting that, in the case of metallizations connected to ports, ∂S_p denotes the boundary of S_p, but the port segment $\overline{\partial S}_p$.

IV. Coupling and Port Integrals

When considering metallic areas with a rectangular shape, the coupling integrals (6) and the port integrals (7) can be calculated analytically by using the analytical expressions of the basis functions (see, for instance, [10]). This possibility is precluded in the case of arbitrary shapes because the basis functions are determined numerically. In this case, the surface integration (6) is a time-consuming task, especially in cases of basis functions determined by a boundary integral method, since it requires the numerical evaluation of the basis functions in many points within the integration domain S_p. However, the coupling integrals (6) can be transformed from surface to line integrals, thus dramatically reducing the computing time. As shown in the Appendix, we have

$$\int_{S_p} \vec{e}_r'^{(p)} \cdot \vec{\mathcal{E}}_m' \, dS = 0 \tag{20}$$

$$\int_{S_p} \vec{e}_r''^{(p)} \cdot \vec{\mathcal{E}}_m' \, dS = \frac{\kappa_r''^{(p)}}{k_m' \left(\kappa_r''^{(p)2} - k_m'^2 \right)} \int_{\partial S_p} \psi_r''^{(p)} \frac{\partial \chi_m'}{\partial n_p} \, d\ell \tag{21}$$

$$\int_{S_p} \vec{e}_r^{\,0(p)} \cdot \vec{\mathcal{E}}_m' \, dS = 0 \tag{22}$$

$$\int_{S_p} \vec{e}_r'^{(p)} \cdot \vec{\mathcal{E}}_m'' \, dS = \frac{k_m''}{\kappa_r'^{(p)} \left(\kappa_r'^{(p)2} - k_m''^2 \right)} \int_{\partial S_p} \chi_m'' \frac{\partial \psi_r'^{(p)}}{\partial n_p} \, d\ell \tag{23}$$

$$\int_{S_p} \vec{e}_r''^{(p)} \cdot \vec{\mathcal{E}}_m'' \, dS = \frac{1}{\kappa_r''^{(p)} k_m''} \int_{\partial S_p} \psi_r''^{(p)} \frac{\partial \chi_m''}{\partial t_p} \, d\ell \tag{24}$$

$$\int_{S_p} \vec{e}_r^{\,0(p)} \cdot \vec{\mathcal{E}}_m'' \, dS = -\frac{1}{k_m''} \int_{\partial S_p} \chi_m'' \frac{\partial \psi_r^{0(p)}}{\partial n_p} \, d\ell \tag{25}$$

where $\partial / \partial t_p$ is the derivative along the boundary, namely, in the direction of $\vec{t}_p = \vec{u}_z \times \vec{n}_p$.

It is noted that these formulas hold true in both cases of metallizations connected or not connected to ports.

For the port integrals (7), we easily obtain

$$\int_{\overline{\partial S}_p} \vec{e}_r''^{(p)}(\vec{r}) \cdot (-\vec{n}_p) \, d\ell = 0 \tag{26}$$

$$\int_{\overline{\partial S}_p} \vec{e}_r''^{(p)}(\vec{r}) \cdot (-\vec{n}_p) \, d\ell = \frac{1}{\kappa_r''^{(p)}} \int_{\overline{\partial S}_p} \frac{\partial \psi_r''^{(p)}}{\partial n_p} \, d\ell \tag{27}$$

$$\int_{\overline{\partial S}_p} \vec{e}_r^{\,0(p)}(\vec{r}) \cdot (-\vec{n}_p) \, d\ell = 0. \tag{28}$$

V. Application of the BI–RME Method

In the analysis of circuits of practical interest, some tens of basis functions (8) and (9) are usually needed for each metallic area. This, in turn, requires the calculation of some tens of eigensolutions of Helmholtz equations (10) and (11).

In the past years, some of the authors developed a novel method (i.e., the BI–RME method) for the solution of the Helmholtz equation in arbitrary domains [17]–[19]. A comprehensive description of the BI–RME method is reported in [11]. In this section, we limit ourselves to a brief outline of the BI–RME method, to highlight its advantages in the calculation of entire domain basis functions.

The BI–RME method is a modified boundary integral approach for the evaluation of eigenfunctions. The surface S_p (either simply or multiply connected) is considered as a part of a fictitious enlarged domain Ω_p with a rectangular shape [see Fig. 3(a)]. The eigenfunctions to be determined are defined in Ω_p, and are assumed to vanish outside S_p. They are expressed as combinations of boundary integrals (BIs) and a resonant mode expansion (RME), involving the modal potentials of the region Ω_p. The boundary integrals involve $\partial \psi_r'^{(p)} / \partial n_p$ and $\psi_r''^{(p)}$ over the line σ_p [see Fig. 3(a)], which corresponds to the part of ∂S_p not coincident with the rectangular boundary. Using

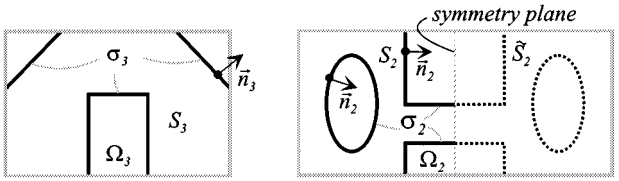

(a) (b)

Fig. 3. Geometry for the application of the BI–RME method. (a) Internal metallic area. (b) Metallic area connected to a port.

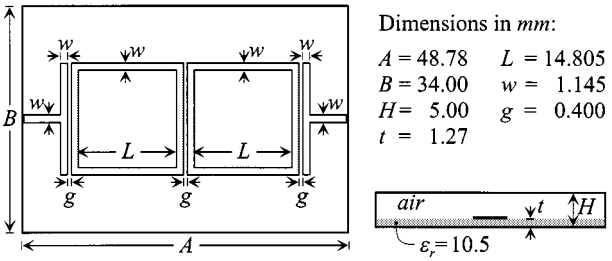

Fig. 4. Printed microstrip filter composed of T-shaped port elements and square-loop resonators.

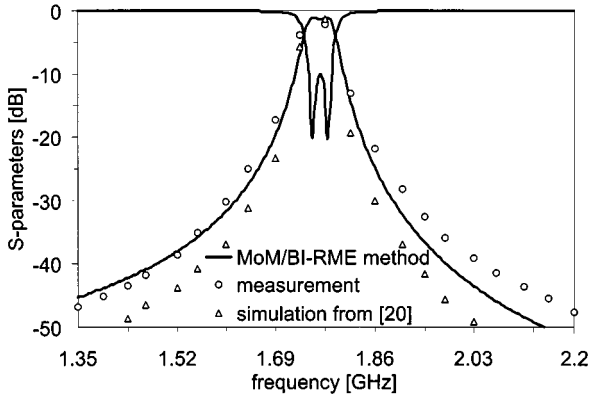

Fig. 5. Comparison between simulated and measured results presented in [20], and results obtained with the present approach, for the filter shown in Fig. 4.

the BI–RME representation of the eigenfunctions and imposing the proper boundary conditions on σ_p, the eigenvalue problems (10) and (11) are converted into integral-differential equations. As in the case of the conventional boundary element method (BEM), the discretized problem resulting from the application of the BI–RME method is much smaller than in conventional approaches based on differential equations (finite element method (FEM), finite-difference time-domain (FDFD), etc.). Differently from the conventional BEM, the BI–RME method leads to the determination of the eigenfunctions by the solution of a linear matrix eigenvalue problem. In particular, it provides as eigenvalues $\kappa_r^{\prime(p)}$ and $\kappa_r^{\prime\prime(p)}$ up to a prescribed value $\kappa_{\max}$, and as eigenfunctions $\partial\psi_r^{\prime(p)}/\partial n_p$ and $\psi_r^{\prime\prime(p)}$ over the line σ_p and the modal amplitudes of the RME.

The method is very efficient and reliable, also in cases where a large number of eigenfunctions have to be determined. Moreover, no spurious modes are found. Furthermore, it is worth noting that the order of the matrix eigenvalue problem to be solved depends on the extension of the line σ_p and of the surface of the resonator Ω_p. For this reason, the efficiency of the BI–RME method highly improves when a large part of the boundary of S_p fits with the rectangular boundary, as in the example in Fig. 3(a).

The evaluation of coupling integrals (21), (23), and (24) requires $\partial\psi_r^{\prime(p)}/\partial n_p$ and $\psi_r^{\prime\prime(p)}$ on ∂S_p. On the portion σ_p, these quantities are directly the solutions of the BI–RME method. On the other part of ∂S_p, they are obtained from the BI–RME representation of the eigenfunctions (see [11, eqs. (5.44) and (5.94)]). Even if a post-processing is required for obtaining the boundary values on $\partial S_p - \sigma_p$, it is convenient to let ∂S_p coincide with $\partial\Omega_p$ as much as possible. In fact, this reduces the dimensions of the eigenvalue problems to be solved, thus increasing the rapidity and accuracy of the solution.

To solve the Helmoltz equation in the case of a metallization connected to a port, the exterior domain Ω_p includes not only S_p, but also its mirror image $\tilde{S}_p$, as shown in Fig. 3(b). The problem is solved by imposing an even or an odd symmetry condition with respect to the symmetry plane shown in Fig. 3(b). The details on the implementation of the BI–RME method taking into account the symmetries are discussed in [11, Sec. 5.2.3].

Finally, for multiply connected surfaces, all the possible basis functions (12) must be considered, requiring the determination of all the solutions $\psi_r^{0(p)}$ of the Laplace equation (13). These basis functions are obtained by solving (13) through the conventional BEM [17]. Even in this case, when the patch is connected to a port, it is possible to solve the Laplace equation by creating a mirror image $\tilde{S}_p$ of S_p, and considering an even symmetry condition on the symmetry plane.

VI. Numerical Results

We used the code for the analysis of printed circuits involving resonators with complex shapes, which fully exploit the capabilities of the method.

The first example refers to the analysis of a narrow-band microstrip filter composed of two T-shaped port elements and two square-loop resonators (Fig. 4), firstly proposed in [20]. The results obtained by the MoM/BI–RME approach are reported in Fig. 5 and compared with experimental data and simulations given in [20], showing a good agreement. The convergence was obtained with 4000 modes of the box and 62 basis functions (eight on each T-shaped line and 23 on each loop resonator), corresponding to $\kappa_{\max} = 1.153\,\mathrm{mm}^{-1}$.

For this example, we report in Fig. 6 the study of the convergence properties of the MoM/BI–RME method. In particular, we verified the convergence when varying the number of basis functions [see Fig. 6(a)], and when varying the number of modes of the box [see Fig. 6(b)]. These graphs show that the frequency response does not change when considering more than 62 basis functions or more than 4000 modes of the box.

The calculation of the frequency response of Fig. 5 takes 22 s for the determination of the basis functions and the evaluation of the coupling and port integrals, and 0.135 s for the MoM solution in each frequency point (on a Pentium III at 1 GHz). Thus, the total computing time for the analysis in 100 frequency points is 35.5 s. It is worth observing that taking advantage of the symmetries of the geometry (which were not exploited in

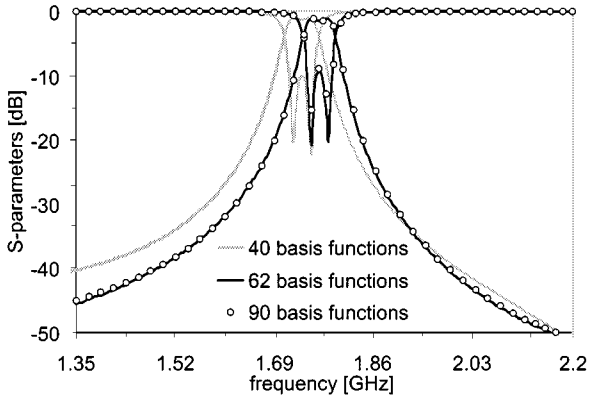

(a)

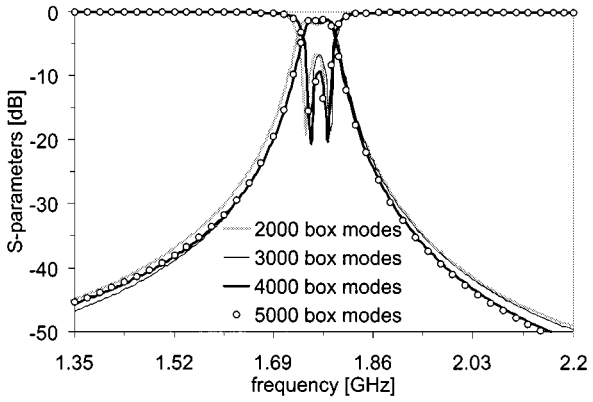

(b)

Fig. 6. Convergence behavior of the MoM/BI–RME method in the analysis of the circuit shown in Fig. 4. (a) As a function of the total number of basis functions, when considering 4000 modes of the box. (b) As a function of the number of modes of the box, when considering 62 basis functions.

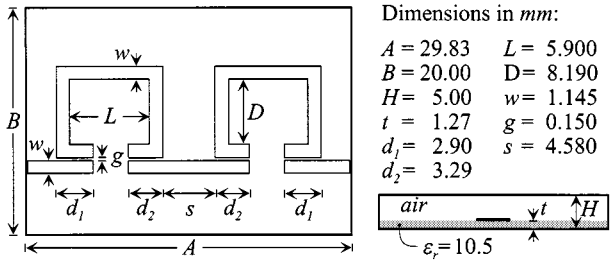

Fig. 7. Printed microstrip filter composed of two open-loop resonators.

our analysis) should lead to a dramatic reduction of the total computing time.

The second example refers to the analysis of a narrow-band microstrip filter composed of two open-loop resonators (Fig. 7) [20]. The analysis of this structure (already presented in [12]) is particularly challenging since the lines and loops are separated by very narrow capacitive gaps, and the surface current must be accurately represented near these gaps. Consequently, in this case, the analysis requires more basis functions than in the previous example. Fig. 8 shows the frequency response of the filter considering 4000 modes of the box and 158 basis functions (12 on each port line, 22 on the middle line, and 56 on each open loop) corresponding to $\kappa_{\max} = 3.144\,\mathrm{mm}^{-1}$. The results are in a good agreement with the theoretical and experimental data taken from [20]. The computing time (without exploiting the

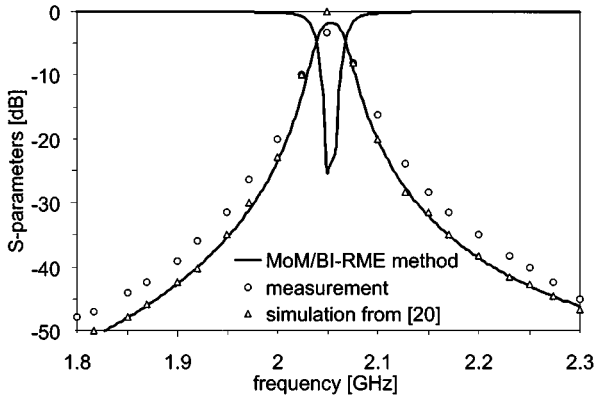

Fig. 8. Comparison between simulated and measured results presented in [20], and results obtained with the present approach, for the filter shown in Fig. 7.

symmetries) is 48 s for the calculation of the basis functions and of the coupling and port integrals, and 0.63 s for the MoM solution in each frequency point (on a Pentium III at 1 GHz). Thus, the total computing time for the analysis in 100 frequency points is 111 s.

As a final remark, we can observe that the selection of the basis functions in our approach is performed by a spectral criterion, including all the entire domain basis functions up to a prescribed $\kappa_{\max}$. Especially in cases of metallizations where one of the dimensions is much larger than the other (e.g., narrow strips), this criterion leads to the adoption of very large values of $\kappa_{\max}$, in order to include in the set of basis functions a sufficient number of elements with significant variation along the narrow dimension. Of course, it can happen that many basis functions with uselessly rapid variation in the larger direction can be included in the basis. These functions could be discarded, but the procedure for their recognition is too complicate to be conveniently implemented in a general purpose computer code. Anyway, the numerical experiments presented above permit not to dramatize the problem because we noted that it is sufficient to consider basis functions whose variation in the narrow dimension correspond to one or two sinusoidal oscillations. In spite of the roughness of the current representation, the results are very good: i.e., probably dependent on the variational properties of the admittance parameters obtained by the Galerkin procedure.

VII. Conclusion

We have presented an efficient technique for the accurate analysis of shielded multilayered printed circuits composed of arbitrarily shaped metallic areas. This technique is based on an IE solved by using the MoM with entire domain basis functions. The basis functions are efficiently evaluated by the BI–RME method. This leads to MoM matrices of small size, even in the case of complex circuits. Moreover, the transformation of the coupling integrals from surface to line integrals permits to use the basic outputs of the BI–RME method for calculating the MoM matrix.

The analyzes of circuits of practical interest have been reported and compared with both theoretical and experimental data, showing that the approach is indeed feasible and leads to a software code, which is both efficient and accurate.

APPENDIX

Following a procedure similar to the one presented in [21], [22], the transformation of the coupling integrals from surface to line integrals is based on the application of Green's identity (see, for instance, [23, Appendix 2, eq. 45])

$$\int_{S_p} \vec{\mathcal{A}} \cdot \nabla_T \mathcal{B}\, dS = \int_{\partial S_p} \mathcal{B}\vec{n} \cdot \vec{\mathcal{A}}\, d\ell + \int_{\overline{\partial S}_p} \mathcal{B}\vec{n} \cdot \vec{\mathcal{A}}\, d\ell - \int_{S_p} \mathcal{B}\nabla_T \cdot \vec{\mathcal{A}}\, dS. \quad \text{(A.1)}$$

In the case of internal patches, obviously, the port segment $\overline{\partial S}_p$ is not defined and the line integral on $\overline{\partial S}_p$ vanishes.

Derivation of (20)

The electric modal fields are related to scalar potentials through (8) and (3), thus resulting in

$$\int_{S_p} \vec{e}_r^{\,\prime(p)} \cdot \vec{\mathcal{E}}'_m\, dS = \int_{S_p} \vec{u}_z \times \frac{\nabla_T \psi_r^{\prime(p)}}{\kappa_r^{\prime(p)}} \cdot \frac{\nabla_T \chi'_m}{k'_m}\, dS = -\frac{1}{\kappa_r^{\prime(p)} k'_m} \int_{S_p} \nabla_T \psi_r^{\prime(p)} \cdot \vec{u}_z \times \nabla_T \chi'_m\, dS. \quad \text{(A.2)}$$

By applying (A.1) to (A.2) with $\vec{\mathcal{A}} = \vec{u}_z \times \nabla_T \chi'_m$ and $\mathcal{B} = \psi_r^{\prime(p)}$, we have

$$\int_{S_p} \vec{e}_r^{\,\prime(p)} \cdot \vec{\mathcal{E}}'_m\, dS = -\frac{1}{\kappa_r^{\prime(p)} k'_m} \int_{\partial S} \psi_q^{\prime(p)} \vec{n}_p \cdot \vec{u}_z \times \nabla_T \chi'_m\, d\ell - \frac{1}{\kappa_r^{\prime(p)} k'_m} \int_{\overline{\partial S}_p} \psi_q^{\prime(p)} \vec{n}_p \cdot \vec{u}_z \times \nabla_T \chi'_m\, d\ell + \frac{1}{\kappa_r^{\prime(p)} k'_m} \int_{S_p} \psi_r^{\prime(p)} \nabla_T \cdot (\vec{u}_z \times \nabla_T \chi'_m)\, dS. \quad \text{(A.3)}$$

On the right-hand side of (A.3), the surface integral vanishes because of

$$\nabla_T \cdot (\vec{u}_z \times \nabla_T \mathcal{F}) = 0 \quad \text{(A.4)}$$

for any scalar function $\mathcal{F}$ (see, for instance, [23, Appendix 2, eq. 38]), whereas the line integral on ∂S_p vanishes since $\psi_r^{\prime(p)} = 0$ on ∂S_p. Moreover, the line integral on $\overline{\partial S}_p$ is not defined for internal patches and, in the case of patches attached to ports, it vanishes since $\vec{n}_p \cdot \vec{u}_z \times \nabla_T \chi'_m = -\partial \chi'_m / \partial t_p = 0$ on $\overline{\partial S}_p$. This proves (20).

Derivation of (21)

From (9) and (3), we have

$$\int_{S_p} \vec{e}_r^{\,\prime\prime(p)} \cdot \vec{\mathcal{E}}'_m\, dS = \int_{S_p} \frac{\nabla_T \psi_r^{\prime\prime(p)}}{\kappa_r^{\prime\prime(p)}} \cdot \frac{\nabla_T \chi'_m}{k'_m}\, dS = \frac{1}{\kappa_r^{\prime\prime(p)} k'_m} \int_{S_p} \nabla_T \psi_r^{\prime\prime(p)} \cdot \nabla_T \chi'_m\, dS. \quad \text{(A.5)}$$

By applying (A.1) to (A.5) with $\vec{\mathcal{A}} = \nabla_T \chi'_m$ and $\mathcal{B} = \psi_r^{\prime\prime(p)}$, and using the Helmoltz equation $\nabla_T^2 \chi'_m = -k_m^{\prime 2} \chi'_m$, we have

$$\int_{S_p} \vec{e}_r^{\,\prime\prime(p)} \cdot \vec{\mathcal{E}}'_m\, dS = \frac{1}{\kappa_r^{\prime\prime(p)} k'_m} \int_{\partial S_p} \psi_r^{\prime\prime(p)} \vec{n}_p \cdot \nabla_T \chi'_m\, d\ell + \frac{1}{\kappa_r^{\prime\prime(p)} k'_m} \int_{\overline{\partial S}_p} \psi_r^{\prime\prime(p)} \vec{n}_p \cdot \nabla_T \chi'_m\, d\ell + \frac{k'_m}{\kappa_r^{\prime\prime(p)}} \int_{S_p} \psi_r^{\prime\prime(p)} \chi'_m\, dS. \quad \text{(A.6)}$$

By remembering that $\psi_r^{\prime\prime(p)} = 0$ on $\overline{\partial S}_p$, the line integral on $\overline{\partial S}_p$ in (A.6) vanishes.

Moreover, by applying (A.1) to (A.5) with $\vec{\mathcal{A}} = \nabla_T \psi_r^{\prime\prime(p)}$ and $\mathcal{B} = \chi'_m$, and taking into account that $\nabla_T^2 \psi_r^{\prime\prime(p)} = -\kappa_r^{\prime\prime(p)2} \psi_r^{\prime\prime(p)}$, we have

$$\int_{S_p} \vec{e}_r^{\,\prime\prime(p)} \cdot \vec{\mathcal{E}}'_m\, dS = \frac{1}{\kappa_r^{\prime\prime(p)} k'_m} \int_{\partial S_p} \chi'_m \vec{n}_p \cdot \nabla_T \psi_r^{\prime\prime(p)}\, d\ell + \frac{1}{\kappa_r^{\prime\prime(p)} k'_m} \int_{\overline{\partial S}_p} \chi'_m \vec{n}_p \cdot \nabla_T \psi_r^{\prime\prime(p)}\, d\ell + \frac{\kappa_r^{\prime\prime(p)}}{k'_m} \int_{S_p} \psi_r^{\prime\prime(p)} \chi'_m\, dS. \quad \text{(A.7)}$$

By remembering that $\partial \psi_r^{\prime\prime(p)} / \partial n_p = 0$ on ∂S_p and that $\chi'_m = 0$ on $\overline{\partial S}_p$, the line integrals in (A.7) vanish. Therefore, by substituting the surface integral on the right-hand side of (A.6) into (A.7), and considering $\kappa_r^{\prime\prime(p)2} \neq k_m^{\prime 2}$, we finally obtain (21).

Derivation of (22)

From (12) and (3), we have

$$\int_{S_p} \vec{e}_r^{\,0(p)} \cdot \vec{\mathcal{E}}'_m\, dS = \int_{S_p} \vec{u}_z \times \nabla_T \psi_r^{0(p)} \cdot \frac{\nabla_T \chi'_m}{k'_m}\, dS = \frac{1}{k'_m} \int_{S_p} \nabla_T \psi_r^{0(p)} \cdot \nabla_T \chi'_m \times \vec{u}_z\, dS. \quad \text{(A.8)}$$

By applying (A.1) to (A.8) with $\vec{\mathcal{A}} = \nabla_T \chi'_m \times \vec{u}_z$ and $\mathcal{B} = \psi_r^{0(p)}$, we have

$$\int_{S_p} \vec{e}_r^{\,0(p)} \cdot \vec{\mathcal{E}}'_m\, dS = \frac{1}{k'_m} \int_{\partial S_p} \psi_r^{0(p)} \vec{n}_p \cdot \nabla_T \chi'_m \times \vec{u}_z\, d\ell + \frac{1}{k'_m} \int_{\overline{\partial S}_p} \psi_r^{0(p)} \vec{n}_p \cdot \nabla_T \chi'_m \times \vec{u}_z\, d\ell - \frac{1}{k'_m} \int_{S_p} \psi_r^{0(p)} \nabla_T \cdot (\nabla_T \chi'_m \times \vec{u}_z)\, dS. \quad \text{(A.9)}$$

On the right-hand side of (A.9), the surface integral vanishes due to (A.4). With regard to the line integral on ∂S_p, $\psi_r^{0(p)} = \text{cost}$ on each contour ∂S_p^i. In the case of a closed contour ∂S_p^i

$$\int_{\partial S_p^i} \vec{n}_p \cdot \nabla_T \chi'_m \times \vec{u}_z\, d\ell = \int_{\partial S_p^i} \nabla_T \chi'_m \cdot \vec{t}_p\, d\ell = 0 \quad \text{(A.10)}$$

(see [23, Appendix 2, eq. 55]). In the case of an open line ∂S_p^i (only for patches attached to ports)

$$\int_{\partial S_p^i} \vec{n}_p \cdot \nabla_T \chi_m' \times \vec{u}_z \, d\ell = \int_{\partial S_p^i} \nabla_T \chi_m' \cdot \vec{t}_p \, d\ell = \chi_m'(P) - \chi_m'(Q) \qquad \text{(A.11)}$$

where P and Q are extreme points of the line ∂S_p^i, which are located on the box wall ∂S_{box}, where $\chi_m' = 0$. Finally, the line integral on $\overline{\partial S}_p$ vanishes since $\vec{n}_p \cdot \nabla_T \chi_m' \times \vec{u}_z = \partial \chi_m' / \partial t_p = 0$ on $\overline{\partial S}_p$. This proves (22).

Derivation of (23)

From (8) and (4), we have

$$\int_{S_p} \vec{e}_r^{\,\prime(p)} \cdot \vec{\mathcal{E}}_m'' \, dS = \int_{S_p} \left(\vec{u}_z \times \frac{\nabla_T \psi_r^{\prime(p)}}{\kappa_r^{\prime(p)}} \right) \cdot \left(\frac{\nabla_T \chi_m''}{k_m''} \times \vec{u}_z \right) dS = -\frac{1}{\kappa_r^{\prime(p)} k_m''} \int_{S_p} \nabla_T \psi_r^{\prime(p)} \cdot \nabla_T \chi_m'' \, dS. \qquad \text{(A.12)}$$

Therefore, the derivation of (23) is similar to the one of (21), only taking into account the different boundary condition of the scalar potential $\psi_r^{\prime(p)}$.

Derivation of (24)

From (9) and (4), we have

$$\int_{S_p} \vec{e}_r^{\,\prime\prime(p)} \cdot \vec{\mathcal{E}}_m'' \, dS = \int_{S_p} \frac{\nabla_T \psi_r^{\prime\prime(p)}}{\kappa_r^{\prime\prime(p)}} \cdot \left(\frac{\nabla_T \chi_m''}{k_m''} \times \vec{u}_z \right) dS = \frac{1}{\kappa_r^{\prime\prime(p)} k_m''} \int_{S_p} \nabla_T \psi_r^{\prime\prime(p)} \cdot \nabla_T \chi_m'' \times \vec{u}_z \, dS. \qquad \text{(A.13)}$$

By applying (A.1) to (A.13) with $\vec{\mathcal{A}} = \nabla_T \chi_m'' \times \vec{u}_z$ and $\mathcal{B} = \psi_r^{\prime\prime(p)}$, we have

$$\int_{S_p} \vec{e}_r^{\,\prime\prime(p)} \cdot \vec{\mathcal{E}}_m'' \, dS = \frac{1}{\kappa_r^{\prime\prime(p)} k_m''} \int_{\partial S_p} \psi_r^{\prime\prime(p)} \, \vec{n}_p \cdot \nabla_T \chi_m'' \times \vec{u}_z \, d\ell + \frac{1}{\kappa_r^{\prime\prime(p)} k_m''} \int_{\overline{\partial S}_p} \psi_r^{\prime\prime(p)} \vec{n}_p \cdot \nabla_T \chi_m'' \times \vec{u}_z \, d\ell - \frac{1}{\kappa_r^{\prime\prime(p)} k_m''} \int_{S_p} \psi_r^{\prime\prime(p)} \, \nabla_T \cdot (\nabla_T \chi_m'' \times \vec{u}_z) \, dS. \qquad \text{(A.14)}$$

On the right-hand side of (A.14), the surface integral vanishes due to (A.4). In the case of patches connected to ports, the line integral on $\overline{\partial S}_p$ vanishes since $\psi_r^{\prime\prime(p)} = 0$ on $\overline{\partial S}_p$. Moreover, in the line integral ∂S_p, $\vec{n}_p \cdot \nabla_T \chi_m'' \times \vec{u}_z = \nabla_T \chi_m'' \cdot \vec{t}_p$. This proves (24).

Derivation of (25)

From (12) and (4), we have

$$\int_{S_p} \vec{e}_r^{\,0(p)} \cdot \vec{\mathcal{E}}_m'' \, dS = \int_{S_p} \left(\vec{u}_z \times \nabla_T \psi_r^{0(p)} \right) \cdot \left(\frac{\nabla_T \chi_m''}{k_m''} \times \vec{u}_z \right) dS = -\frac{1}{k_m''} \int_{S_p} \nabla_T \psi_r^{0(p)} \cdot \nabla_T \chi_m'' \, dS. \qquad \text{(A.15)}$$

By applying (A.1) to (A.15) with $\vec{\mathcal{A}} = \nabla_T \psi_r^{0(p)}$ and $\mathcal{B} = \chi_m''$, we have

$$\int_{S_p} \vec{e}_r^{\,0(p)} \cdot \vec{\mathcal{E}}_m'' \, dS = \frac{1}{k_m''} \int_{\partial S_p} \chi_m'' \, \vec{n}_p \cdot \nabla_T \psi_r^{0(p)} \, d\ell + \frac{1}{k_m''} \int_{\overline{\partial S}_p} \chi_m'' \, \vec{n}_p \cdot \nabla_T \psi_r^{0(p)} \, d\ell - \frac{1}{k_m''} \int_{S_p} \chi_m'' \nabla_T^2 \psi_r^{0(p)} \, dS. \qquad \text{(A.16)}$$

On the right-hand side of (A.16), the surface integral vanishes because $\nabla_T^2 \psi_r^{0(p)} = 0$, whereas the line integral on $\overline{\partial S}_p$ vanishes since $\partial \psi_r^{0(p)} / \partial n_p = 0$ on $\overline{\partial S}_p$. This proves (25).

REFERENCES

[1] T. Ishikawa and E. Yamashita, "Experimental evaluation of basic circuit components using buried microstrip lines for constructing high-density microwave integrated circuits," *IEEE Trans. Microwave Theory Tech.*, vol. 44, pp. 1074–1080, July 1996.

[2] H. Okazaki and T. Hirota, "Multilayer MMIC broad-side coupler with a symmetric structure," *IEEE Microwave Guided Wave Lett.*, vol. 7, pp. 145–146, June 1997.

[3] J.-S. Hong and M. J. Lancaster, "Aperture-coupled microstrip open-loop resonators and their applications to the design of novel microstrip bandpass filters," *IEEE Trans. Microwave Theory Tech.*, vol. 47, pp. 1848–1855, Sept. 1999.

[4] J.-Y. Lee, T.-S. Horng, and N. G. Alexopoulos, "Analysis of cavity-backed aperture antennas with a dielectric overlay," *IEEE Trans. Antennas Propagat.*, vol. 42, pp. 1556–1562, Nov. 1994.

[5] L. P. Dunleavy and P. B. Katehi, "A generalized method for analyzing shielded thin microstrip discontinuities," *IEEE Trans. Microwave Theory Tech.*, vol. 36, pp. 1758–1766, Dec. 1988.

[6] G. V. Eleftheriades, J. R. Mosig, and M. Guglielmi, "A fast integral equation technique for shielded planar circuits defined on nonuniform meshes," *IEEE Trans. Microwave Theory Tech.*, vol. 44, pp. 2293–2296, Dec. 1996.

[7] A. Hill and V. K. Tripathi, "An efficient algorithm for the three-dimensional analysis of passive microstrip components and discontinuities for microwave and millimeter-wave integrated circuits," *IEEE Trans. Microwave Theory Tech.*, vol. 39, pp. 83–91, Jan. 1991.

[8] S. M. Rao, D. R. Wilton, and A. W. Glisson, "Electromagnetic scattering by surfaces of arbitrary shape," *IEEE Trans. Antennas Propagat.*, vol. AP-30, pp. 409–418, May 1982.

[9] N. Kinayman and M. I. Aksun, "Efficient use of closed-form Green's functions for the analysis of planar geometries with vertical connections," *IEEE Trans. Microwave Theory Tech.*, vol. 45, pp. 593–603, May 1997.

[10] A. Alvarez Melcón, J. R. Mosig, and M. Guglielmi, "Efficient CAD of boxed microwave circuits based on arbitrary rectangular elements," *IEEE Trans. Microwave Theory Tech.*, vol. 47, pp. 1045–1058, July 1999.

[11] G. Conciauro, M. Guglielmi, and R. Sorrentino, *Advanced Modal Analysis.* New York: Wiley, 2000, ch. 5.

[12] M. Bozzi, L. Perregrini, A. Alvarez Melcon, M. Guglielmi, and G. Conciauro, "MoM/BI–RME analysis of boxed microwave circuits based on arbitrarily shaped elements," in *IEEE MTT-S Int. Microwave Symp. Dig.*, Phoenix, AZ, May 20–25, 2001, pp. 1925–1928.

[13] J. C. Rautio and R. F. Harrington, "An electromagnetic time–harmonic analysis of shielded microstrip circuits," *IEEE Trans. Microwave Theory Tech.*, vol. MTT-35, pp. 726–730, Aug. 1987.

[14] G. V. Eleftheriades and J. R. Mosig, "On the network characterization of planar passive circuits using the method of moments," *IEEE Trans. Microwave Theory Tech.*, vol. 44, pp. 438–445, Mar. 1996.

[15] L. B. Felsen and N. Marcuvitz, *Radiation and Scattering of Waves.* Englewood Cliffs, NJ: Prentice-Hall, 1973.

[16] G. Conciauro and M. Bressan, "Singularity expansion of mode voltages and currents in a layered anisotropic dispersive medium included between two ground planes," *IEEE Trans. Microwave Theory Tech.*, vol. 47, pp. 1617–1626, Sept. 1999.

[17] G. Conciauro, M. Bressan, and C. Zuffada, "Waveguide modes via an integral equation leading to a linear matrix eigenvalue problem," *IEEE Trans. Microwave Theory Tech.*, vol. MTT-32, pp. 1495–1504, Nov. 1984.
[18] G. Conciauro, P. Arcioni, M. Bressan, and L. Perregrini, "Wide-band modeling of arbitrarily shaped H-plane waveguide components by the 'boundary integral-resonant mode expansion method'," *IEEE Trans. Microwave Theory Tech.*, vol. 44, pp. 1057–1066, July 1996.
[19] P. Arcioni, M. Bressan, G. Conciauro, and L. Perregrini, "Wide-band modeling of arbitrarily shaped E-plane waveguide components by the 'boundary integral-resonant mode expansion method'," *IEEE Trans. Microwave Theory Tech.*, vol. 44, pp. 2083–2092, Nov. 1996.
[20] C.-C. Yu and K. Chang, "Novel compact elliptic-function narrow-band bandpass filters using microstrip open-loop resonators with coupled and crossing lines," *IEEE Trans. Microwave Theory Tech.*, vol. 46, pp. 952–958, July 1998.
[21] G. G. Gentili, "Properties of TE–TM mode-matching techniques," *IEEE Trans. Microwave Theory Tech.*, vol. 39, pp. 1669–1673, Sept. 1991.
[22] P. Guillot, P. Couffignal, H. Baudrand, and B. Theron, "Improvement in calculation of some surface integrals: Application to junction characterization in cavity filter design," *IEEE Trans. Microwave Theory Tech.*, vol. 41, pp. 2156–2160, Dec. 1993.
[23] J. Van Bladel, *Electromagnetic Fields*. Bristol, PA: Hemisphere, 1985.

Maurizio Bozzi (S'98–M'00) was born in Voghera, Italy, in 1971. He received the Laurea degree in electronic engineering and the Ph.D. degree in electronics and computer science from the University of Pavia, Pavia, Italy, in 1996 and 2000, respectively.

From December 1996 to September 1997, he was a Guest Researcher at the Technische Universität Darmstadt, Darmstadt, Germany, where he was involved within the framework of a European Training and Mobility of Researchers (TMR) Project. Since 1997, he has been with the Department of Electronics, University of Pavia. His main research activities concern the electromagnetic modeling of frequency-selective surfaces, quasi-optical frequency multipliers, and microwave printed and integrated circuits.

Dr. Bozzi is a member of the Society of Photo-Optical Instrumentation Engineers (SPIE). He is a correspondent of the International Union of Radio Science (URSI). He serves on the Editorial Board of the IEEE TRANSACTIONS ON MICROWAVE THEORY AND TECHNIQUES. He was the recipient of the Microwave Engineering Center for Space Application (MECSA) Prize for the best paper presented by a young researcher at the 2000 Italian Conference on Electromagnetics (XIII RINEM).

Luca Perregrini (M'98) was born in Sondrio, Italy, in 1964. He received the Electronic Engineering degree and Ph.D. degree in electronics and computer science from the University of Pavia, Pavia, Italy, in 1989 and 1993, respectively.

In 1992, he joined the Department of Electronics, University of Pavia, as an Assistant Professor in electromagnetics, and has taught a course in electromagnetic field theory since 1996. His current research interests are in numerical methods for the analysis and optimization of waveguide circuits, electromagnetic modeling of quasi-optical circuits (frequency multipliers and frequency-selective surfaces) in the millimeter-wave and sub-millimeter-wave range, and modeling of microwave printed and integrated circuits.

Alejandro Alvarez Melcón (M'99) was born in Madrid, Spain, in 1965. He received the Ingeniero Superior de Telecomunicaciones degree from the Polytechnic University of Madrid (UPM), Madrid, Spain, in 1991, and the Ph.D. degree in electrical engineering from the Swiss Federal Institute of Technology, Lausanne, Switzerland, in 1998.

In 1988, he joined the Signal, Systems, and Radiocommunications Department, UPM, as a Research Student, where he was involved in the design, testing, and measurement of broad-band spiral antennas for electromagnetic measurements support (EMS) equipment. From 1991 to 1993, he was with the Radio Frequency Systems Division, European Space Agency–European Space Research and Technology Centre (ESA/ESTEC), Noordwijk, The Netherlands, where he was involved in the development of analytical and numerical tools for the study of waveguide discontinuities, planar transmission lines, and microwave filters. From 1993 to 1995, he was with the Space Division, Industry Alcatel Espacio, Madrid, Spain, and was also with the ESA, where he collaborated in several ESA/ESTEC contracts. From 1995 to 1999, he was with the Swiss Federal Institute of Technology, École Polytechnique Fédérale de Lausanne, Lausanne, Switzerland, where he was involved in the field of microstrip antennas and printed circuits for space applications. In 2000, he joined the Polytechnic University of Carthagena, Cartagena, Spain, where he is currently involved with teaching and research activities.

Dr. Melcón was the recipient of the Journee Internationale de Nice sur les Antennes (JINA) Best Paper Award for the best contribution to the JINA'98 International Symposium on Antennas, and the Colegio Oficial Español de Ingenieros de Telecomunicación/Asociación Española de Ingenieros de Telecomunicación (COIT/AEIT) Award for the best Ph.D. thesis in basic information and communication technologies.

Marco Guglielmi (M'78–SM'97) was born in Rome, Italy, on December 17, 1954. He received the Laurea degree in ingegneria elettronica from the University of Rome "La Sapienza," Rome, Italy, in 1979, attended the Scuola di Specializzazione in Elettromagnetismo Applicato, in 1980, received the M.S. degree in electrical engineering from the University of Bridgeport, Bridgeport, CT, in 1982, and the Ph.D. degree in electrophysics from the Polytechnic University of Brooklyn, Brooklyn, NY, in 1986.

From 1984 to 1986, he was an Academic Associate at the Polytechnic University, and from 1986 to 1988, he was an Assistant Professor. From 1988 to 1989, he was an Assistant Professor at the New Jersey Institute of Technology, Newark, NJ. In 1989, he joined the European Space Research and Technology Centre, Noordwijk, The Netherlands, where he is currently the Head of the Technology Strategy Section.

Dr. Guglielmi was the recipient of a 1981 Fulbright Scholarship and a Halsey International Scholarship Program (HISP) Scholarship.

Giuseppe Conciauro (A'72–M'87) was born in Palermo, Italy, in 1937. He received the electrical engineering degree and Libera Docenza degree from the University of Palermo, Palermo, Italy, in 1961 and 1971, respectively.

From 1963 to 1971, he was an Assistant Professor of microwave theory at the Institute of Electrical Engineering, University of Palermo. In 1971, he joined the Department of Electronics, University of Pavia, Pavia, Italy, where he was an Associate Professor, and since 1980, where he has been a Full Professor of electromagnetic theory. From 1985 to 1991, he served as the Director of the Department of Electronics, University of Pavia. He authored *Introduzione alle Onde Elettromagnetiche*(Milano, Italy: McGraw-Hill Italia, 1992) and co-authored *Advanced Modal Analysis*(New York: Wiley, 2000). His main research interests are in microwave theory, interaction structures for particle accelerators, and numerical methods in electromagnetics.

Prof. Conciauro serves on the Editorial Board of the IEEE TRANSACTIONS ON MICROWAVE THEORY AND TECHNIQUES.